

Output Force Enhancement of Finger-type Manipulator by Adopting Brushless DC Motors for Sliding Actuation

Young June Shin, Ho Ju Lee, Kyung-Soo Kim*, Soohyun Kim

Department of Mechanical Engineering, KAIST, Daejeon, 305-701, Republic of Korea

Abstract In this paper, we newly develop a finger-type manipulator driven by the sliding actuation with miniaturized brushless DC (BLDC) motors. The mechanism allows the usage of the maximal capacity of actuators by employing the distributed actuation principle while maintaining the small size. Thanks to the high thrust force of the BLDC motors, the maximum fingertip force of the developed robot finger is remarkably enhanced. Through experimentation, the fingertip force of the proposed robot finger is assessed and compared with the former version with the ultrasonic motors.

Keywords Distributed Actuation, Sliding Actuation, Robot Finger, High Fingertip Force, Robot Manipulator

1. Introduction

The hand is one of the most important parts of the human body, and the high functionality of hands allows a number of delicate tasks, such as the grasp, lifting, or manipulation of objects. The uniqueness of human hands has been recognized and discussed extensively in the literature [1-3]. Likewise, a dexterous robot hand is necessary for various applications such as the end-effector of industrial manipulators, prosthetics, surgical robots, and surveillance robots.

Artificial robot hands commonly adopt electrically geared motors for actuation. For example, DLR-HIT hand II [7], KH hand [8], and the smart hand [9] utilize several electrical motors for dexterous motions together with complicated torque transmission mechanisms.

In [6], the excessive weight of a robot hand is one of the main hindrances for use as a prosthetic device. To overcome the disadvantages of the robot hands driven by electrical motors, light weight actuators, such as a shape memory alloy (SMA) wire, can be adopted for prosthetic hands [10, 11]. An SMA wire has a large power density, but the absolute contraction force may not be sufficient to generate a large grasping force. Also, the slow response due to the heating and cooling processes, and low strain [11] is the typical drawbacks of SMA wires.

Robot hands using pneumatic muscle actuators have been proposed in [12-14]. These robot hands may generate larger power per weight than the SMA wire based robot hands do. However, for generating a large grasping force, a large

capacity compressor should be employed to produce high pressure. Recently, in [16], a DC motor and an SMA wire were combined for the robot hand. In [15], the robot finger utilizing the stacked EAP actuator is also proposed.

Despite efforts to develop anthropomorphic hands, the performance, such as the grasping force with respect to the size or weight, may not be satisfactory today. To address this problem, the distributed (or sliding) actuation principle was proposed in [4]. It utilizes the spatial freedom of the actuation location as an additional design parameter to maximize the fingertip force of the robot finger. The fingertip force was shown to be widely adjustable by only controlling the positions of the sliders.

However, the use of ultrasonic motors leads to absolutely small fingertip force. Motivated by the weakness of [4], in this paper, to enhance the maximum fingertip force, we newly developed a robot finger driven by tiny BLDC motors based on the distributed actuation mechanism.

By optimizing the positions of the sliders, the fingertip force can be remarkably increased. To verify the effectiveness of the idea, simulation and experiments are performed. The paper is organized as follows. In Section II, the distributed actuation principle is shortly revisited and the BLDC motor driven manipulator is newly introduced. Section III is devoted to numerically assessing the performance of the developed robot finger. Section IV describes the experimental results. Finally, conclusions are drawn in Section V.

2. Development of Robot Finger

2.1. Distributed Actuation Mechanism

Based on the observations of human finger muscles, the distributed actuation mechanism was proposed in [4]. The

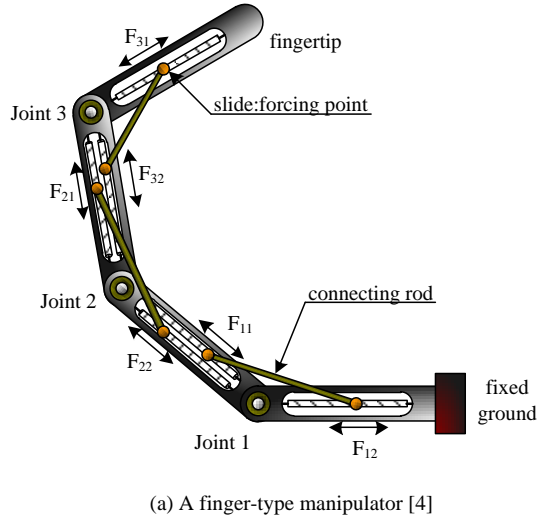
* Corresponding author:

kyungsookim@kaist.ac.kr (Kyung-Soo Kim)

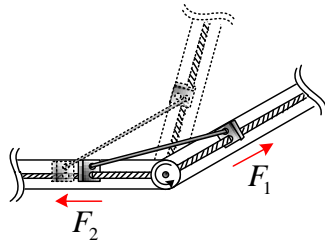
Published online at <http://journal.sapub.org/jmea>

Copyright © 2012 Scientific & Academic Publishing. All Rights Reserved

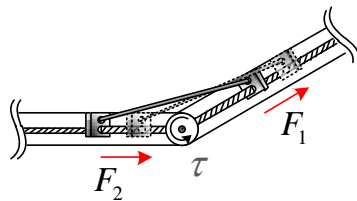
muscles distributed on each phalange of a finger play an important role of multiple actuations for bending or extending the finger. To abstract the features of muscles in a human finger, the mechanism is effectively implemented as shown in Fig. 1(a). A slider can move along a link, and two sliders at each joint are connected by a connecting rod at each joint. Therefore, by changing the positions of the sliders, the desired joint angle can be achieved, as shown in Fig. 1(b). Also, in particular, the sliders may be relocated along the links while the joint angle is fixed as shown in Fig. 1(c). It would give a different joint torque. This allows an additional design factor to optimize the joint torque at each joint. This feature was verified by the simulation and experiments in [4], in which an earlier version of finger-type manipulator I (FM I) was reported. The structure of FM I adopting tiny ultrasonic motors results in a robot finger design of small size and light weight. However, the fingertip force of FM I is very small due to the small thrust forces of ultrasonic motors.



(a) A finger-type manipulator [4]



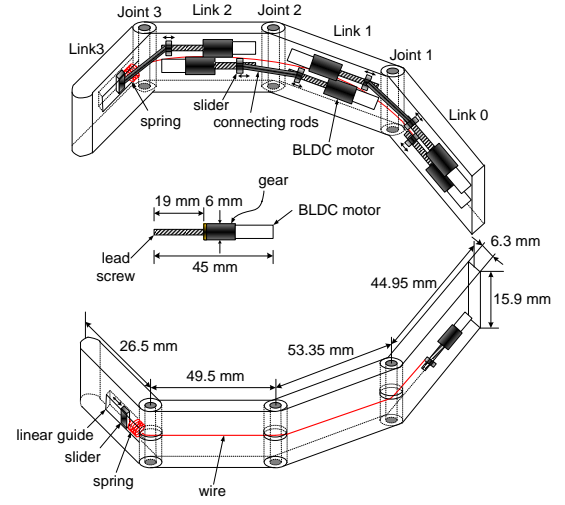
(b) Bending motion at a joint



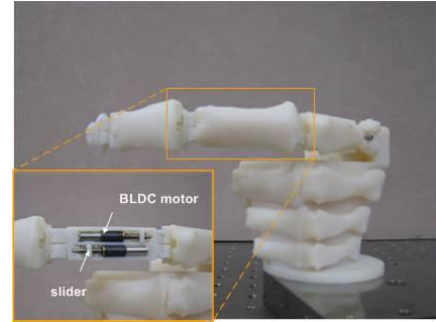
(c) Relocation of sliders without changing the joint angle

Figure 1. A concept of a distributed actuation mechanism

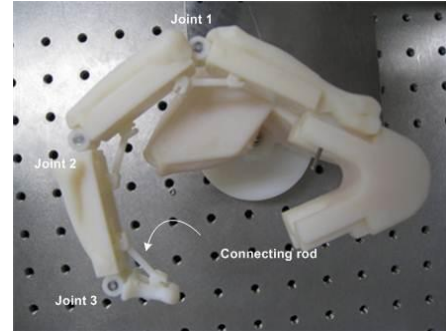
2.2. BLDC Motor-based Design



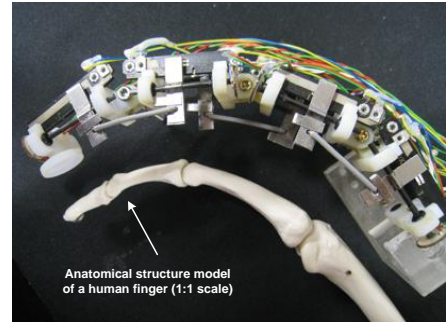
(a) Inner structure of FM II



(b) Front view of FM II



(c) Top view of FM II



(d) FM I [4]

Figure 2. Comparison of two developed robot fingers

To overcome the shortcoming of FM I, we newly designed a finger-type manipulator, the so-called FM II, by embedding the BLDC motors, as shown in Fig. 2(a) [5]. FM II consists of four links with three joints. The linear motions of sliders can be achieved by the miniaturized BLDC motors with lead screws, except for the slider of Link 3. Note that, due to the short length of Link 3, the slider is wired to and driven by the motor at Link 0. Also, by using a tensile spring, the slider can be pushed away. The connecting rods are for connecting two sliders around a joint. The motor has a gear with a ratio of 1:125, a diameter of 6 mm, and a maximum torque of 0.0190 Nm.

According to [19], the thrust forces of sliders can be calculated by

$$F_t = \frac{2\tau}{d_m} \left(\frac{\pi d_m - \mu l}{l + \pi \mu d_m} \right)$$

Where l is the lead pitch, d_m is the mean diameter of the lead screw, μ is the Coulomb friction coefficient, and t is the motor torque. With the values such that $l = 1$ mm, $d_m = 3$ mm, $\mu = 1.45$, and $t = 0.0190$ Nm, the maximal thrust force is calculated with 6.87N.

For the exterior shape similar to a human finger, the three-dimensional profiles (STL model) for each phalange of the middle finger bone model were obtained by using the 3D laser scanning device (Vivid 9i, Konica Minolta Sensing, Inc.). Then, the data was converted to a solid model by using 3-D CAD programs (Rapid Form, CATIA P3V5R17). Then, using a rapid prototype machine (Object Eden 330), we manufactured a robot finger frame and the components, such as the connecting rods and the sliders, as shown in Figs. 2(b) and (c). The design parameters for FM II are summarized in Table 1 in comparison to FM I (shown in Fig. 2(d)). Because of the usage of BLDC motors, the weight of FM II was increased, but the thrust force of sliders was remarkably enhanced by 12.8 times. Note that the movable range of the sliders is restricted within 12 mm, which allows a joint angle between 0° to 90° .

Table 1. Design parameters of the developed fingers

Items	Finger-type manipulator I [5]	Finger-type Manipulator II
Size(mm)	12(H) x 20(W) x 110(L)	6.3(H) x 15.9(W) x 176.0(H)
Weight(gf)	14.7	33.4
Actuators	Ultrasonic motor (Piezo-Technology Co. Ltd.)	Brushless DC motor, $\phi 6$, 3.5gf (Faulhaber Corp.)
Thrust force(N)	0.537 N	6.87
Degree of freedom	3 DOF (four links with three joints)	
Joint angle range	$0^\circ < \theta_j < 90^\circ, j=1,2,3$	

3. Assessment of Finger-Type Manipulator II

In this section, the fingertip force of FM II is assessed by simulations. As shown in Fig. 3, the fingertip force is defined in a normal direction and can be computed by

$$f(\theta_1, x_s) \triangleq |F \cdot n| \quad (1)$$

Where θ_1 is the angle at Joint 1, $x_s = [x_{11}, x_{21}, x_{31}]^T$ is the position vector of independent sliders, n is the unit normal vector, and F is calculated by using the Jacobian matrix [5] (see Appendix for details). For simplicity, it is assumed that $F_{j2} = 0$ so that the sliders with x_{11} , x_{21} , and x_{31} move independently with specified thrust forces.

Note that, in (1), the normal force can be expressed only with a joint angle θ_1 and the slider positions x_s . In Fig. 3, one may observe that, given a fixed end-point at (13.9 mm, 113.7 mm), the joint angles θ_2 and θ_3 should be uniquely determined if θ_1 is fixed. This implies that θ_1 is a single parameter to determine the posture of FMII. Now, even with a fixed posture of FM II, the sliders may have different locations, denoted by x_s . This clearly shows that the fingertip force varies depending on the location of the sliders, which was called the distributed actuation effect in (1).

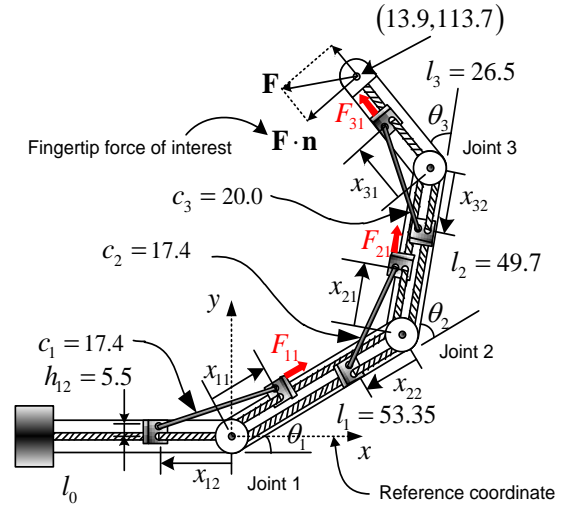


Figure 3. Notations of common parameters for simulation (all in the mm units)

The calculation results of fingertip force with the values in Table 2 are shown in Fig. 4, and the important aspects of FM II can be summarized as follows:

- The redundancy of posture allows a various range of fingertip force. Observe that the maximum curve significantly increases by simply changing the posture of FM II (i.e., through θ_1).
- The distributed actuation provides an additional design freedom to maximize the fingertip force of FMII. For instance, at a fixed posture (e.g. $\theta_1 = 70^\circ$), the fingertip

force varies from 1.67 N to 2.22 N by relocating the sliders. This means that the fingertip force can be maximized by optimizing the slider positions at a specific posture.

- Moreover, the distributed actuation enables a wide range of fingertip force control. For example, if we fix a posture at $q_1 = 70^\circ$, the fingertip force can be controlled between 1.67N and 2.22N by changing the sliders. This feature can be adopted for a delicate force control when grasping fragile objects.

Table 2. Summary of common simulation parameters ($(x_e, y_e) = 13.9$ mm, 113.7 mm)

Items	Specifications
Link, l_j (mm)	$l_1=53.35, l_2=49.7, l_3=26.5$
Connecting rod, c_j (mm)	$c_1=c_2=17.4, c_3=20$
Friction coefficient	$\mu_{11} = \mu_{21} = \mu_{31} = 1.45$
Thrust force, F_{j1} (N)	$F_{11} = F_{21} = F_{31} = 6.87$
Thrust force, F_{j2} (N)	$F_{12} = F_{22} = F_{32} = 0$
Mechanical offset $h_{jk}, j = 1,2,3, k = 1,2$	$h_{11} = h_{21} = h_{31} = 5.5,$ $h_{12} = h_{22} = h_{32} = 5.5$

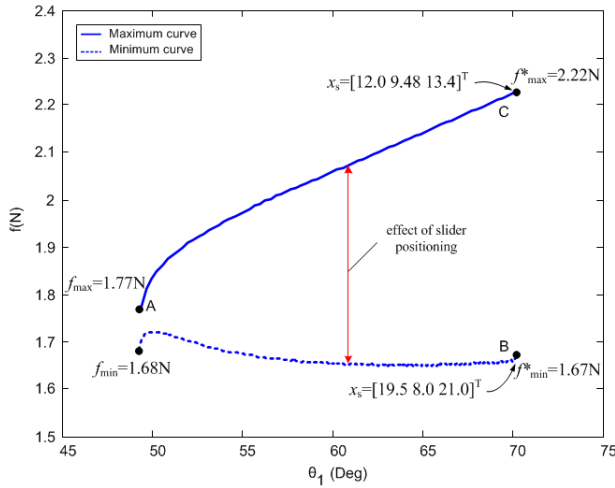


Figure 4. Fingertip force of FM II depending on θ_j and x_s (A, B, and C denotes the cases that will be tested experimentally)

4. Experiments

4.1. Description of Experiments

To verify the performance of FM II having sliders with high thrust forces, we measured the fingertip force under the experimental environment as shown in Fig. 5. Given a target position, (13.9, 113.7) mm, we selected three different cases, A, B, and C, as marked in Fig. 4 and measured the output forces. The specific conditions for three cases are summarized in Table 3. The fingertip force was measured by a load cell (BCL1kgf, CAS Corp.). To measure the fingertip force, first, the fingertip was located by a position feedback control at the target position. Then, the position control was turned off, and the feed forward control with

constant thrust force was turned on at the target position.

4.2. Experimental Results and Discussions

The measured forces are shown in Fig. 6, and the averaged fingertip forces for 3 seconds between 15 sec and 18 sec are summarized in Table 3. It is noted that the measured fingertip forces approximately match the simulation results.

In fact, the experimental results for the three cases demonstrate the effects of the slider positions and the posture of FM II. As expected in Fig. 4, Case A results in a small fingertip force. However, by changing the posture (at $q_1 = 70.4^\circ$), the fingertip force varies from 1.56N (Case B) to 2.19N (Case C). As a result, in terms of the fingertip force, the redundancy of posture, and distributed actuation by relocating sliders jointly enhance the fingertip force of FM II. These features generically allow the usage of the maximal capacity of the BLDC motors to increase the fingertip force.

Overall, by adopting miniaturized BLDC motors to implement the distributed actuation, the fingertip force has been significantly enhanced by 17.3 times compared with FM I. To demonstrate this, an experiment to lift a weight of 200 gf was conducted, as shown in Fig. 7, and lifting such weight was not possible with FM I. Table 4 summarizes the performance parameters for comparison.

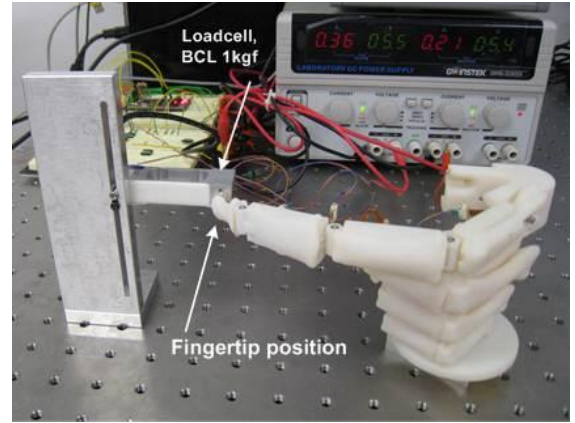


Figure 5. Experimental setup for measurement of fingertip force

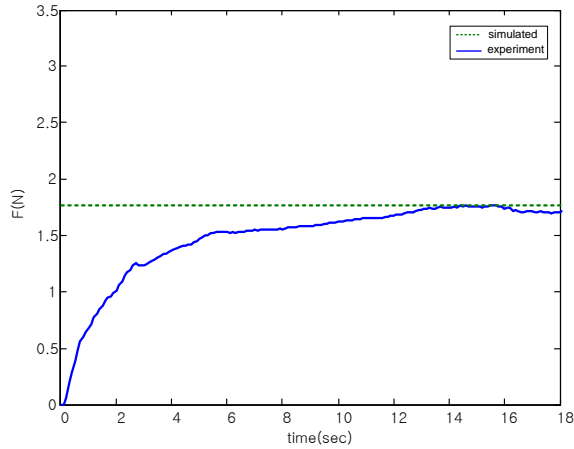
Table 3. Experimental conditions for three cases

Case	Posture & slider		Fingertip force (N)	
			Sim.	Exp.
A	$\theta_1, \theta_2, \theta_3$	49.3°, 56.1°, 1.54°	1.77	1.73
	x_{11}, x_{21}, x_{31}	8.85, 17.0, 10.1		
	x_{12}, x_{22}, x_{32}	5.1, 8.0, 10.1		
B	$\theta_1, \theta_2, \theta_3$	70.4°,0.1°,70.7°	1.67	1.56
	x_{11}, x_{21}, x_{31}	19.5, 8.0, 21.0		
	x_{12}, x_{22}, x_{32}	8.0, 9.36, 10.2		
C	$\theta_1, \theta_2, \theta_3$	70.4°,0.1°,70.7°	2.22	2.19
	x_{11}, x_{21}, x_{31}	12.0, 9.48, 13.4		
	x_{12}, x_{22}, x_{32}	16.8, 8.0, 18.6		

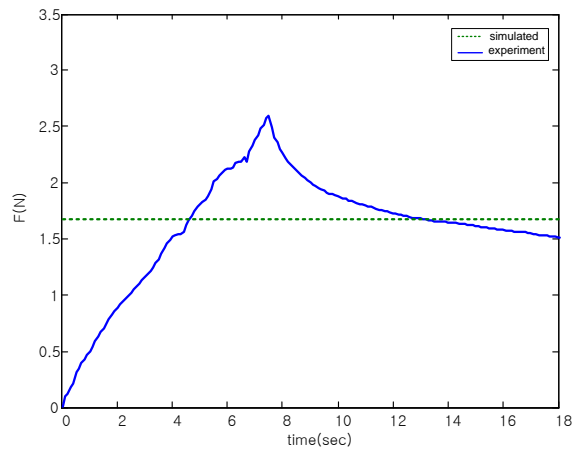
(x_{j1} & x_{j2} denote the target positions of the sliders inmm-unit.)

Table 4. Comparison of fingertip force

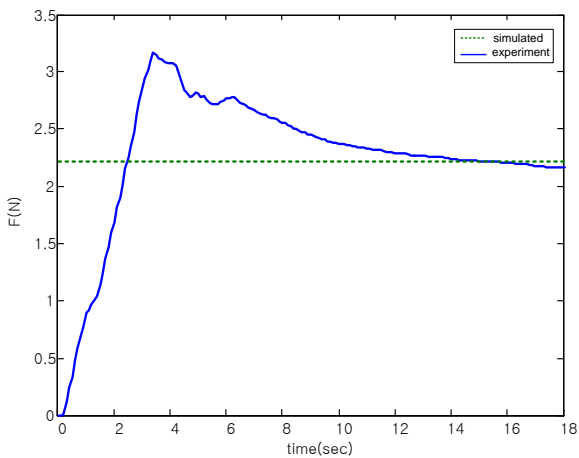
	Finger-type Manipulator I	Finger-type Manipulator II
Maximum thrust force (N)	0.537	6.87
Maximum measured fingertip force (N)	0.126	2.19
An adjustable range of fingertip force (N)	$0.064 < F < 0.126$	$1.67 < F < 2.19$



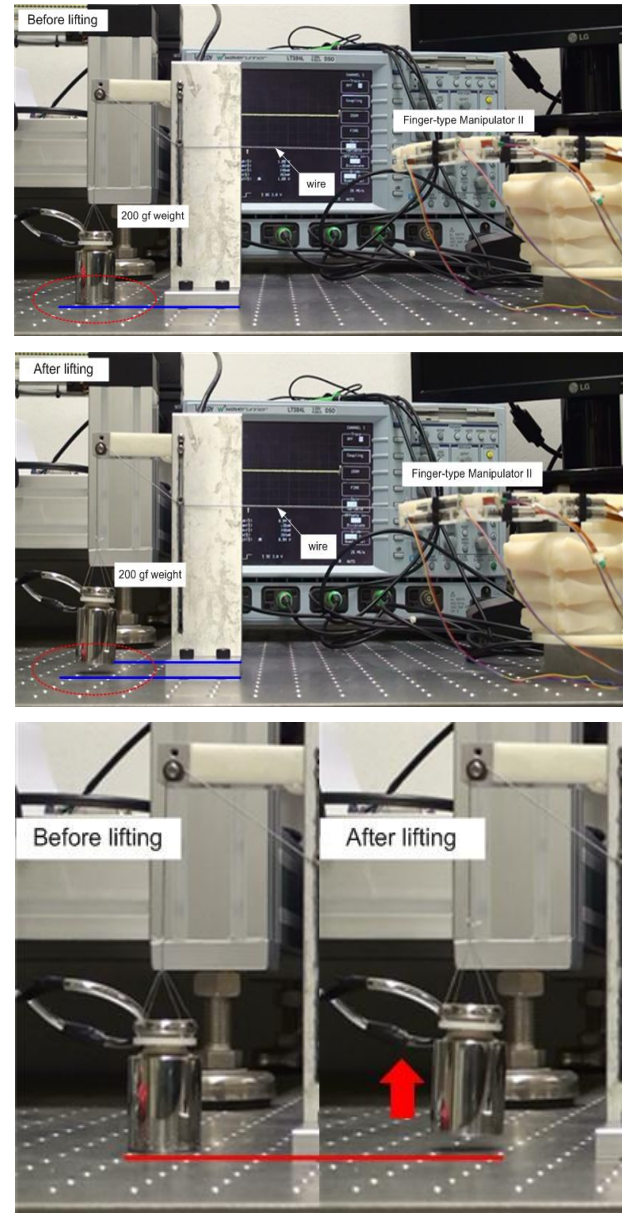
(a) Measured force for Case A



(b) Measured force for Case B



(c) Measured force for Case C

Figure 6. Experimental results for measurement of fingertip force**Figure 7.** Demonstration of fingertip force enhancement by lifting a weight of 200 gf. Before lifting (top), after lifting (middle)

5. Conclusions

In this paper, an improved version of a finger-type manipulator was newly proposed. By implementing the distributed actuation principle with miniaturized BLDC motors, we achieved a high fingertip force while maintaining the light structure. The newly developed robot finger merely weights 33.4 gf, but produces a maximum fingertip force of 2.19 N. Thanks to the large thrust forces of the sliders, the fingertip force increases remarkably compared with the former version. By simulation and experiments, the effect of the distributed actuation principle and the feasibility of the proposed mechanism were verified.

APPENDIX

Derivation of Torque at Joints and Fingertip Force

Let us consider the torques at the joints as follows:

$$\tau_j(F_{j1}, x_{j1}, \theta_1) = F_{j1} \frac{x_{j1} \tan \psi_{j1} + h_{j1}}{1 + \mu_{j1} \tan \psi_{j1}} \quad (\text{A.1})$$

where F_{j1} is the thrust force, x_{j1} is the slider position, and

$$\psi_{j1} = \tan^{-1} \left(\tan \theta_j \sqrt{\frac{c_j^2 - x_j^2 \cos^2 \theta_j}{c_j^2 + x_j^2 \sin^2 \theta_j}} \right)$$

$$\psi_{j2} = \theta_j - \psi_{j1}$$

$x_{j2} = -x_{j1} \cos \theta_j + \sqrt{-x_{j1}^2 \sin^2 \theta_j + c_j^2}$ for $j = 1, 2, 3$. Under the joint torques presented above, the fingertip force can be described by

$$F = \left((JH^{-1}J^T)^{-1} JH^{-1} \right) \tau \quad (\text{A.2})$$

where $\tau := [\tau_1, \tau_2, \tau_3]^T$, and $H \in \mathbf{R}^{3 \times 3}$ and $J \in \mathbf{R}^{2 \times 3}$ are the joint space kinetic energy matrix and the Jacobian matrix, respectively.

ACKNOWLEDGEMENTS

This work was supported by the Unmanned Technology Research Center, Korea Advanced Institute of Science and Technology, originally funded by the Defense Acquisition Program Administration, Agency for Defense Development.

REFERENCES

- [1] Antonio Bicchi, "Hands for Dexterous Manipulation and Robust Grasping: A Difficult Road toward Simplicity," *IEEE Transaction on Robotics and Automation*, vol.16, no.6, pp.652-662, 2000.
- [2] H-L. Yu, R. A. Chase, B. Strauch, *Atlas of Hand Anatomy and Clinical Implications*, St. Louis: Mosby, 2004.
- [3] Z. Yu and J. Gu, "A Survey on Real-time Controlled Multi-fingered Robotic Hand," in *Proceedings of Canadian Conference on Electrical and Computer Engineering*, pp.975-980, 2008.
- [4] Y. J. Shin and K.-S. Kim, "Distributed Actuation Mechanism for a Finger-type Manipulator: Theory & Experiments," *IEEE Transactions on Robotics*, vol.26, no.3, pp.569-575, 2010.
- [5] Y. J. Shin, K.-S. Kim, and S. Kim, "BLDC motor driven robot finger design using the sliding actuation principle," *International Conference on Cybernetics and Intelligent Systems & Robotics, Automation and Mechatronics*, pp. 550-553, 2010.
- [6] L. E. Pezzin, T. R. Dillingham, E. J. MacKenzie, P. Ephraim and P. Rossbach, "Use and satisfaction with prosthetic limb devices and related services," *Archives of Physical Medicine and Rehabilitation*, vol. 85, pp. 368-375, 2004.
- [7] H. Liu, P. Meusel, N. Seitz, B. Willberg, G. Hirzinger, M. H. Jin, Y. W. Liu, R. Wei, and Z. W. Xie, "The modular multisensory DLR-HIT-Hand," *Mechanism and Machine Theory*, vol. 42, no. 5, pp. 612-625, 2007.
- [8] T. Mouri, H. Kawasaki, and K. Umebayashi, "Developments of New Anthropomorphic Robot Hand and its Master Slave System," in *Proceedings of IEEE/RSJ International Conference on Intelligent Robots and Systems*, pp. 3225-3230, 2005.
- [9] C. Cipriani, M. Controzzi, and M. C. Carrozza, "Progress Towards the Development of the Smart-Hand Transradial Prosthesis," in *Proceedings of IEEE 11th International Conference on Rehabilitation Robotics*, pp.682-687, 2009.
- [10] T. Maeno and T. Hino, "Miniature five-fingered robot hand driven by shape memory alloy actuators," in *Proceedings of the 12th IASTED International Conference Robotics and Applications*, pp.174-179, 2006.
- [11] V. Bundhoo, E. Haslam, B. Birch and E. J. Park, "A shape memory alloy-based tendon-driven actuation system for biomimetic artificial fingers, part I: design and evaluation," *Robotica*, vol. 27, no. 1, pp. 131-146, 2009.
- [12] F. Rothling, R. Haschke, J. J. Steil, and H. Ritter, "Platform portable anthropomorphic grasping with the bielefeld 20-DOF shadow and 9-DOFTUM hand," in *Proceedings of IEEE/RSJ International Conference on Intelligent Robots and Systems*, pp. 2951-2956, 2007.
- [13] A. Kargov, C. Pylatiuk, H. Klosek, R. Oberle, and S. Schulz, "Modularly designed lightweight anthropomorphic robot hand," in *Proceedings of IEEE International Conference on Multisensor Fusion and Integration for Intelligent Systems*, pp.155-159, 2006.
- [14] N. Tsujiuchi, T. Koizumi, S. Nishino, H. Komatsubara, T. Kudawara, and M. Hirano, "Development of pneumatic robot hand and construction of master-slave system," *Journal of System Design and Dynamics*, vol.2, no.6, pp. 1306-1315, 2008.
- [15] N. H. Chuc, J. K. Park, N. H. L. Vuong, D. Kim, J. C. Koo, Y. Lee, J.-D. Nam, H. R. Choi, "Multijointed robot finger driven by artificial muscle actuator," in *Proceedings of IEEE International Conference on Robotics and Automation*, pp. 587-592, 2009.
- [16] Josiah B. Rosmarin and H. Harry Asada, "Synergistic Design of a Humanoid Hand with Hybrid DC Motor SMA Array Actuators Embedded in the Palm," in *Proceedings of IEEE International Conference on Robotics and Automation*, pp. 773-778, 2008.
- [17] J. D.W. Madden, N. A. Vandesteeg, P. A. Anquetil, P. G. A. Madden, A. Takshi, R. Z. Pytel, S. R. Lafontaine, P. A. Wieringa, and I. W. Hunter, "Artificial Muscle Technology: Physical Principles and Naval Prospects," *IEEE Journal of Oceanic Engineering*, vol. 29, no. 3, pp. 706-728, 2004.
- [18] R. Balasubramanian and Y. Matsuoka, "Biological stiffness control strategies for the anatomically correct testbed (ACT) hand," in *Proceedings of IEEE International Conference on Robotics & Automation*, pp. 737-742, 2008.
- [19] Shigley, C. R. Mischke, R. G. Budynas, *Mechanical Engineering Design*, New York, US: McGraw Hill, 2003.